Colored Multilayers from Transparent Submicrometer Spheres

C. D. Dushkin,† K. Nagayama,* T. Miwa, and P. A. Kralchevsky†

Protein Array Project, ERATO, JRDC, 5-9-1 Tokodai, Tsukuba, 300-26, Japan

Received October 7, 1992. In Final Form: May 28, 1993®

Ordered multilayers were formed by evaporating the water from polystyrene latex suspensions containing monodisperse spherical particles of diameter smaller than the wavelength of visible light. It was found that multilayers of different thicknesses exhibit different intensive and uniform colors when illuminated with polychromatic light. Their intensity strongly depends on the refractive index of the substrate on which the multilayers are deposited. The colors are due to interference at plane parallel films of different thicknesses. By measuring the wavelengths at which the reflectance of two neighboring multilayers coincide, it is established that the particle array has hexagonal packing. This is in agreement with the data obtained by scanning electron microscopy and atomic force microscopy. Such an ordered multilayer exhibits a stepwise change in its color each time when the upper particle layer is removed. This property could find application for creating and recording color images.

Introduction

Ever since the first optical studies with monodisperse latex suspensions conducted by Alfrey *et al.*,[1] three-color phenomena have been observed. According to Krieger and O'Neill[2] they can be classified as follows: (i) Colors are observed in highly diluted latexes which are attributable to Mie[3] scattering by individual latex particles. (ii) Iridescent colors are observed in relatively concentrated latexes of particle diameter between 0.15 and 0.50 μm. This effect is due to Bragg diffraction from three-dimensional arrays (colloidal crystals) formed inside the suspension;[4] the diffraction pattern has been utilized by a number of authors[5–8] for characterizing the properties of the colloidal crystals. (iii) A different color phenomenon is observed when white light is transmitted through or reflected from an ordered monolayer from latex particles, whose diameters are greater than 0.4 μm. In this case the colors are due to diffraction by two-dimensional (2D) arrays of particles. The latex 2D-arrays can be obtained by compression of a particle monolayer in a Langmuir trough.[8]

Recently we observed another color phenomenon with monodisperse latex particles (55 nm and 144 nm diameters), which is described and investigated in the present article. We formed particle monolayers and multilayers on a transparent substrate (glass or mica), which had been previously coated with thin transparent gold or carbon film. We observed that the multilayers of different thicknesses exhibit different brilliant uniform colors. We found out that the presence of a carbon or gold coating plays a crucial role: the same latex multilayers deposited on a bare glass surface exhibit only a hardly visible coloring, which can be easily overlooked. It turns out that the colors observed by us can be attributed neither to Bragg diffraction as in the experiments[4–8] mentioned above nor to Mie scattering the latter being observed in metallic sols[9,10] and in chromoskedasic painting.[11] In fact, in our case the color stripes are due to interference of light at plane parallel films; see, e.g., refs 12 and 13. A similar phenomenon is observed with stratifying vertical liquid films containing latex particles.[14,15] It is demonstrated below that from the interference data one can extract information about the particle size and ordering.

Experimental Procedure and Observations

Preparation of Particle Multilayers. The ordered multilayers of latex particles have been prepared on horizontal substrates by using an experimental technique described in detail elsewhere.[16,17] In particular, an experimental cell of cylindrical paraffin wall (block of paraffin wax with a cylindrical hole) was used whose bottom was a horizontal transparent plate representing the substrate.[17] The area of the bottom was 3.14 mm^2. In our experiments we loaded the cell with 1-μL drop of aqueous latex suspension (polystyrene latex, JSR, Japan) at initial latex volume fraction 0.001. The suspension covered the bottom of the cell with a layer of average thickness *ca.* 300 μm. The upper surface of this layer was a concave liquid meniscus.

As the water evaporates from the latex suspension layer, its thickness gradually decreases with time. The central part of the concave meniscus first approaches the bottom of the cell thus creating a plane-parallel liquid film over the center of the substrate. When the thickness of this film becomes smaller than the latex particle diameter and the tops of the particles protrude

* Author to whom correspondence should be addressed.
† Permanent address: Laboratory of Thermodynamics and Physico-chemical Hydrodynamics, Faculty of Chemistry, University of Sofia, 1126 Sofia, Bulgaria.

® Abstract published in *Advance ACS Abstracts*, October 15, 1993.

(1) Alfrey, T., Jr.; Bradford, E. B.; Vanderhoff, J. W. *J. Opt. Soc. Am.* **1954**, *44*, 603.
(2) Krieger, I. M.; O'Neill, F. M. *J. Am. Chem. Soc.* **1968**, *90*, 3114.
(3) Mie, G. *Ann. Phys.* **1908**, *25*, 377.
(4) Luck, W.; Klier, M.; Wesslau, H. *Ber. Bunsen-Ges. Phys. Chem.* **1963**, *67*, 75.
(5) Hiltner, P. A.; Krieger, I. M. *J. Phys. Chem.* **1969**, *73*, 2386.
(6) Hiltner, P. A.; Papir, Y. S.; Krieger, I. M. *J. Phys. Chem.* **1971**, *75*, 1881.
(7) Hachisu, S.; Kobayashi, Y.; Kose, A. *J. Colloid Interface Sci.* **1973**, *42*, 342.
(8) Goodwin, J. W.; Ottewill, R. H.; Parentich, A. *J. Phys. Chem.* **1980**, *84*, 1580.
(9) Kruyt, J. R. *Colloid Science*; Elsevier: Amsterdam, 1949.
(10) Shchukin, E. D.; Pertsov, A. V.; Amelina, E. A. *Colloid Chemistry*; Moscow University Press: Moscow, 1982.
(11) Man-Kit Lam, D.; Rossiter, B. W. *Sci. Am.* **1991**, November, 48.
(12) Born, M.; Wolf, E. *Principles of Optics*, 4th ed.; Pergamon Press: Oxford, 1970.
(13) Meyer-Arendt, J. R. *Introduction to the Classical and Modern Optics*; Prentice-Hall: London, 1972; Chapter 2.8.
(14) Nikolov, A. D.; Wasan, D. T.; Kralchevsky, P. A.; Ivanov, I. B. In *Ordering and Organisation in Ionic Solutions*; Ise, N., Sogami, I., Eds.; World Scientific: Teaneck, NJ, 1988; p 302.
(15) Basheva, E. S.; Nikolov, A. D.; Kralchevsky, P. A.; Ivanov, I. B.; Wasan, D. T. In *Surfactants in Solution*; Mittal, K. L., Shah, D. O., Eds.; Plenum Press: New York, 1991; Vol. 11, p 467.
(16) Denkov, N. D.; Velev, O. D.; Kralchevsky, P. A.; Ivanov, I. B.; Yoshimura, H.; Nagayama, K. *Langmuir* **1992**, *8*, 3183.
(17) Dushkin, C. D.; Yoshimura, H.; Nagayama, K. *Chem. Phys. Lett.* **1993**, *204*, 455.

0743-7463/93/2409-3695$04.00/0

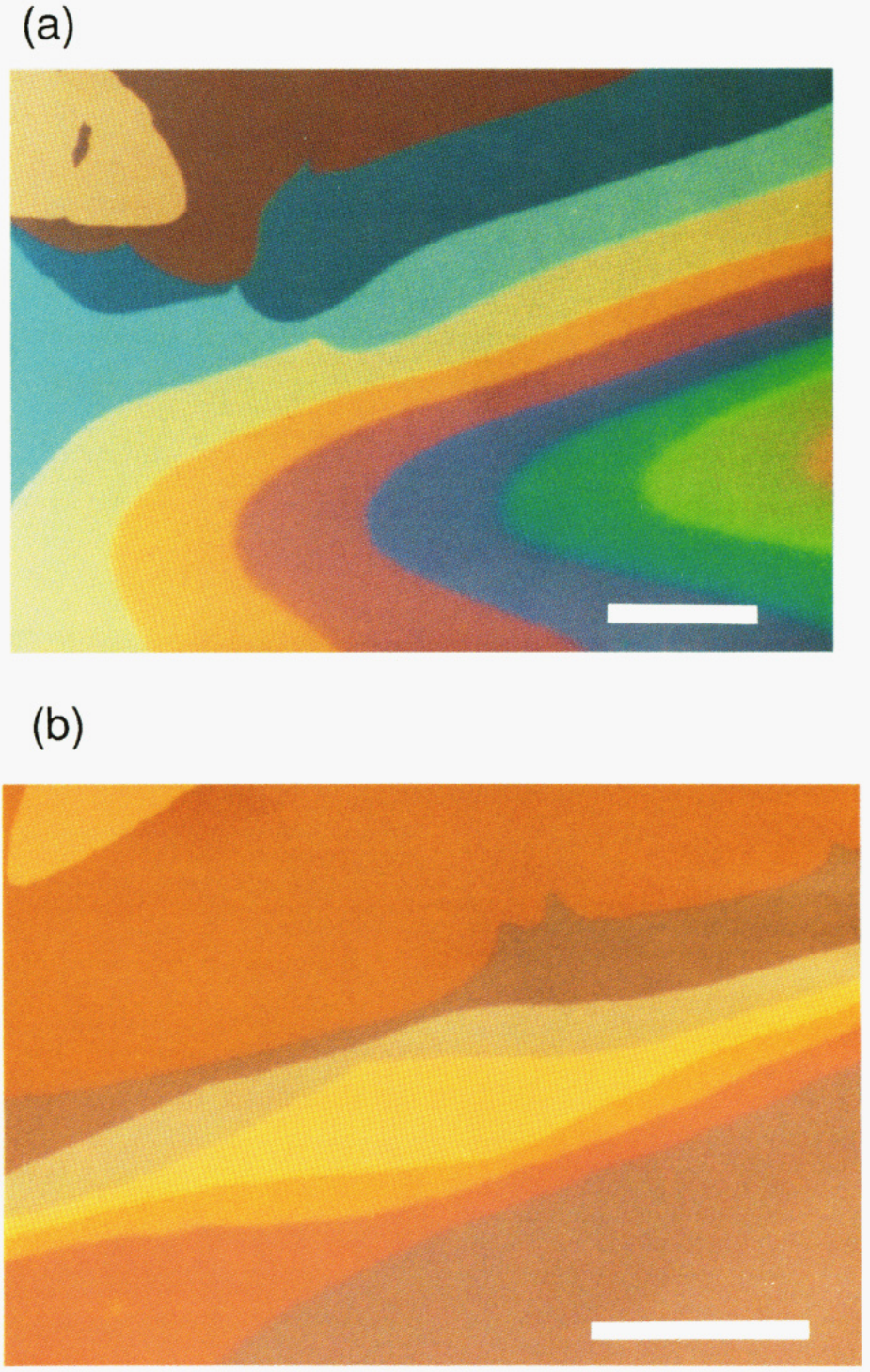

Figure 1. Photographs in light reflected from ordered multilayers of latex particles (55 nm diameter): (a) deposited on gold-coated glass, reference marker 100 μm; (b) carbon-coated glass, reference marker 100 μm. (See also Table I.)

from the water, an ordered 2D-cluster of particles is formed due to the action of attractive lateral capillary forces.[18] This cluster plays the role of a nucleus triggering the formation of an ordered latex particle monolayer.[16,17] The area of the nucleus increases with time because of the attachment of new particles to its periphery. These particles are being brought by an intensive lateral water influx which tends to compensate the water evaporated from the surface of the nucleus.[16] The ordered monolayer or multilayers of particles, thus, concentrically grow toward the cell wall from the central area.[17]

The slope of the concave liquid meniscus encircling the nucleus increases gradually during the growth of the ordered monolayer. At some moment a particle bilayer beings to form as a ring encircling the monolayer. After some time a trilayer starts to form as a ring encompassing the bilayer. Later one can observe consecutive formation of 4-layers, 5-layers, ..., up to 14-layers in some experiments. In an ideal case the consecutive multilayers would resemble the circular rows of an amphitheater with the monolayer in the central area. However, in reality the boundaries between the different multilayers can strongly deviate from circular shape due to some instabilities. As a result, the multilayers appear as stripes of uneven width.

Color Observation. As could be expected, the colors observed in transmitted and reflected light are complementary to each other. For the sake of brevity, we will discuss only colors observed in light reflected from the multilayers. Since the color depends

(18) (a) Kralchevsky, P. A.; Paunov, V. N.; Ivanov, I. B.; Nagayama, K. *J. Colloid Interface Sci.* **1992**, *151*, 79. (b) Kralchevsky, P. A.; Nagayama, K. *Langmuir*, in press.

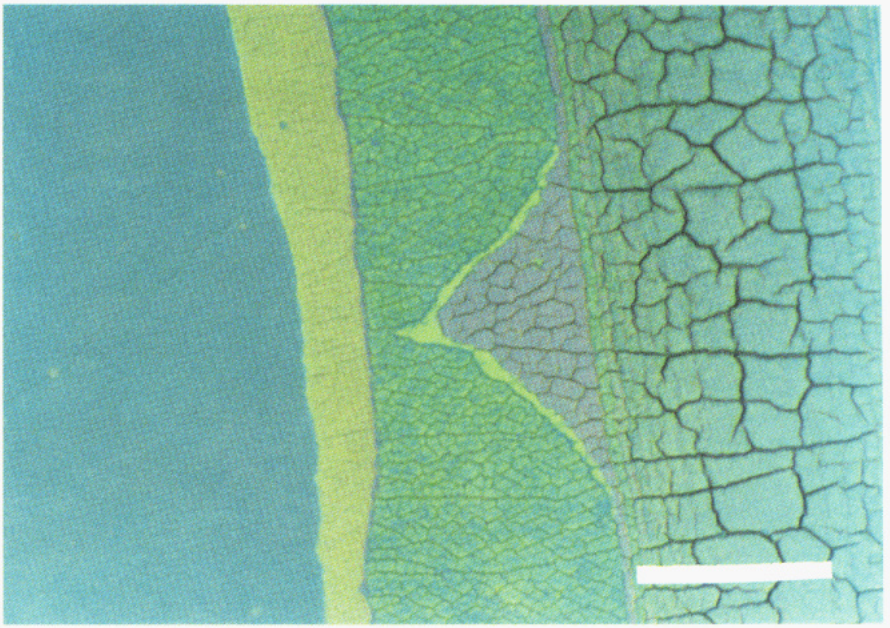

Figure 2. Photograph in light reflected from ordered multilayers of latex particles (144 nm diameter) deposited on a mica plate; length of the reference marker is 50 μm.

Table I. Colors of Dried Latex Particle Multilayers on Gold-Coated Glass

no. of layers k	thickness[a] h_k, nm	color in reflected light[b]	no. of layers k	thickness[a] h_k, nm	color in reflected light[b]
1	47	ochre	7	277	magenta
2	85	brown	8	316	blue-purplish
3	124	navy blue	9	354	green
4	162	sky blue	10	392	yellow-green
5	201	yellow	11	431	orange
6	239	orange	12	469	red

[a] The values of h_k are calculated from eq 10 for perfect hexagonal close packing by using the experimental effective particle diameter d = 47 nm (see Table III). [b] Due to the photograph reproduction, some of the colors in Figure 1 can exhibit different nuances of the true colors listed here.

on the angle of incidence, our considerations below will be specified for the case of normal incidence.

The most pronounced color effect we observed was with a gold-coated glass substrate. Figure 1a represents a photomicrograph in reflected light of the substrate covered with latex particle multilayers of different thicknesses. The diameter of a latex particle is 55 ± 4 nm as determined by the producer. The monolayer is colored ochre, the bilayer is brown, etc. The consequence of the colors is listed in Table I. The same colors, however of lower intensity, are observed with latex particle monolayers of identical thickness prepared on a carbon-coated glass substrate (Figure 1b). The lower intensity can be explained with the lower reflectivity of the carbon-coated glass compared with the gold coated one. It is worthwhile noting that in both cases the stripes exhibit uniform colors and the boundaries between them are sharp.

The multilayers shown in Figure 2 are built up from latex particles of diameter 144 ± 2 nm. The multilayers containing one-, two-, three-, four-, and five-particle layers exhibit respectively blue, ochre, green, red, and brown colors. One sees big cracks, especially in the thicker multilayers. We believe these cracks are due to the drying up of the water from the latex particle multilayers. One sees also that the colors in Figure 2 are not as intensive and brilliant as those in Figure 1. This is due in part to the higher order of interference[13] as well as to the lower reflectivity of the substrate (mica) compared with coated glass.

As mentioned earlier, the dried multilayers built up from a different number of layers exhibit different colors when illuminated with white light and observed by microscope. The effect is hardly visible when the multilayers are formed on a glass substrate (Matsunami optical glass plate washed with chromic acid). When the substrate is mica, the colors become more pronounced. The colors are very well pronounced when the substrate is glass coated with thin carbon or gold film; see Figure 1. In our experiments the coating of thickness about 50 Å was prepared by vacuum evaporation. After that the coated plates were exposed to ion sputtering for 40 s to make the surface more hydrophilic and thus to ensure better spreading of the latex suspension on the substrate. The obtained thin coatings were transparent and allowed observations in both transmitted and reflected light.

Structure of the Latex Multilayers. Since the latex particles used in our experiments are too small (55 and 144 nm) to be observed by an optical microscope, we applied a SEM (scanning electron microscope, JSM-820, JEOL) and AFM (atomic force microscope, SFA-300, Seiko Instr. Inc., Japan) to study the structure of the latex particle multilayers. Figure 3 represents SEM images of particle layers formed by the 144-nm latex. Both the monolayer and the bilayer have hexagonal packing. Dislocations and cracks are also observed. Besides, one observes a curious phenomenon: a narrow band of *tetragonal* packing intervening between two consecutive multilayers of hexagonal packing. In Figure 3b this is a tetragonal bilayer between hexagonal monolayer and bilayer. Similarly, a band of yellow color (tetragonal four-layer) intervenes between the green hexagonal trilayer and the red hexagonal four-layer in Figure 2. Analogous small tetragonal multilayers have been observed with larger (visible) latex particles.[16] The consecutive formation of hexagonal and tetragonal multilayers follows the phase diagram for a system of spheres confined in a narrow slit (with wedge shape).[19,20] In our case, the role of the upper wedge surface is played by the inclined liquid meniscus, which exists during the process of multilayer formation.

An advanced technique developed by Yamaki *et al.*[21] was used for the AFM measurements with 55-nm latex particles; see Figure 4. This technique includes growing of a very sharp electron beam deposited carbon tip in laboratory conditions. (The commercially available tips for AFM do not provide good images of such small particles.) The boundary between a monolayer (darker region) and bilayer (bright region) is observed in Figure 4a. One sees hexagonal packing of the particles in both these regions. However, the structure is not perfect: the brighter and darker specks

(19) Pieranski, P.; Strzelecki, L.; Pansu, B. *Phys. Rev. Lett.* **1983**, *50*, 900.
(20) Pansu, B.; Pieranski, P. *J. Phys.* **1984**, *45*, 331.
(21) Yamaki, M.; Miwa, T.; Yoshimura, H.; Nagayama, K. *J. Vac. Sci. Technol.* **1992**, *B10*, 2447.

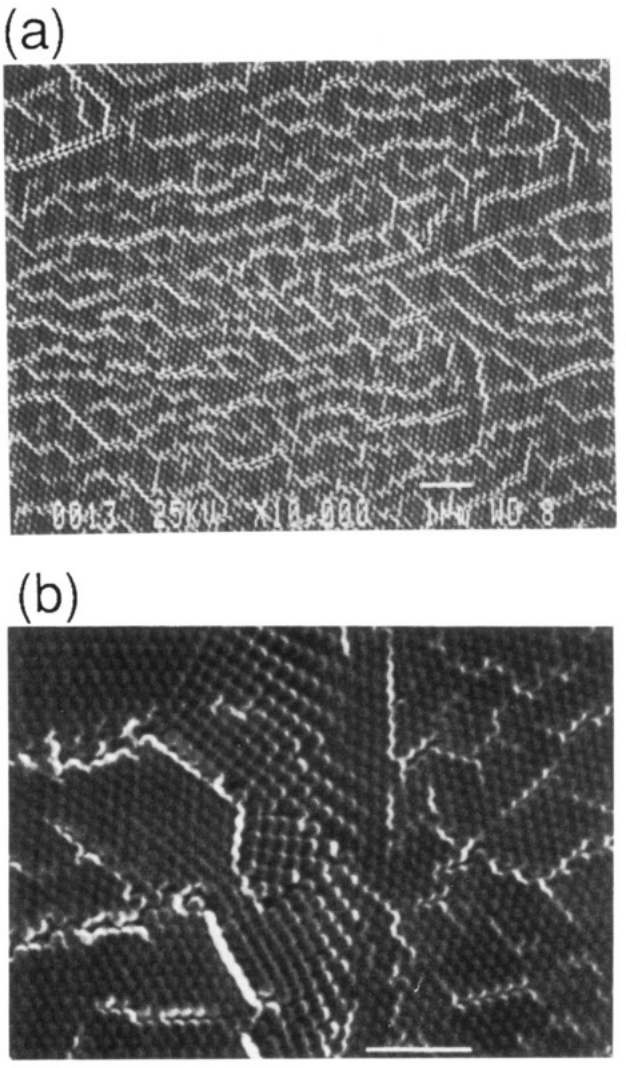

Figure 3. SEM micrographs of layers from latex particles of diameter 144 nm: (a) micrograph of a hexagonal monolayer, reference marker 1 μm; (b) micrograph of a tetragonal bilayer (in the center) between a hexagonal monolayer (on the right) and a hexagonal bilayer (on the left), reference marker 1 μm.

indicate positions in the lattice with larger and smaller thickness, respectively. Since the variations in intensity inside the regions covered by monolayer and bilayer are small compared with the drop of the intensity at the boundary between monolayer and bilayer, one can conclude that the surface roughness is small compared with the particle diameter. In addition, the surface roughness is much smaller than the wave of the visible light. On that reason the color stripes in Figure 1 seem homogeneous. Figure 4b is obtained from an independent AFM scanning of a particle monolayer at higher magnification. The hexagonal packing of particles is more clearly evident, though the surface roughness appears to be more pronounced as holes and hills. This observation implies that the surface roughness of the latex particle layers shown in Figure 4 can be due, at least in part, to the scratching of the particle layers by the tip of the atomic force microscope during the process of scanning.

Interferometric Measurements. The colored multilayers studied by us (see Figures 1 and 2) look like stripes of different intensity when illuminated with *monochromatic* light. If the wavelength of the monochromatic light is varied, one observes that the intensities of two neighboring stripes can coincide at a particular wavelength. The latter can be measured with good precision. The data are presented in Table II, where k denotes the number of layers in a multilayer and $\lambda_{k,k+1}$ is the measured wavelength (*in vacuo*), for which the intensities of the light reflected from the k layer and $(k + 1)$ layer coincide. Usually for a given couple $(k, k + 1)$ one can observe only one $\lambda_{k,k+1}$ and rarely two λ's (see the rows with $k = 5$ and 8 in Table II). The

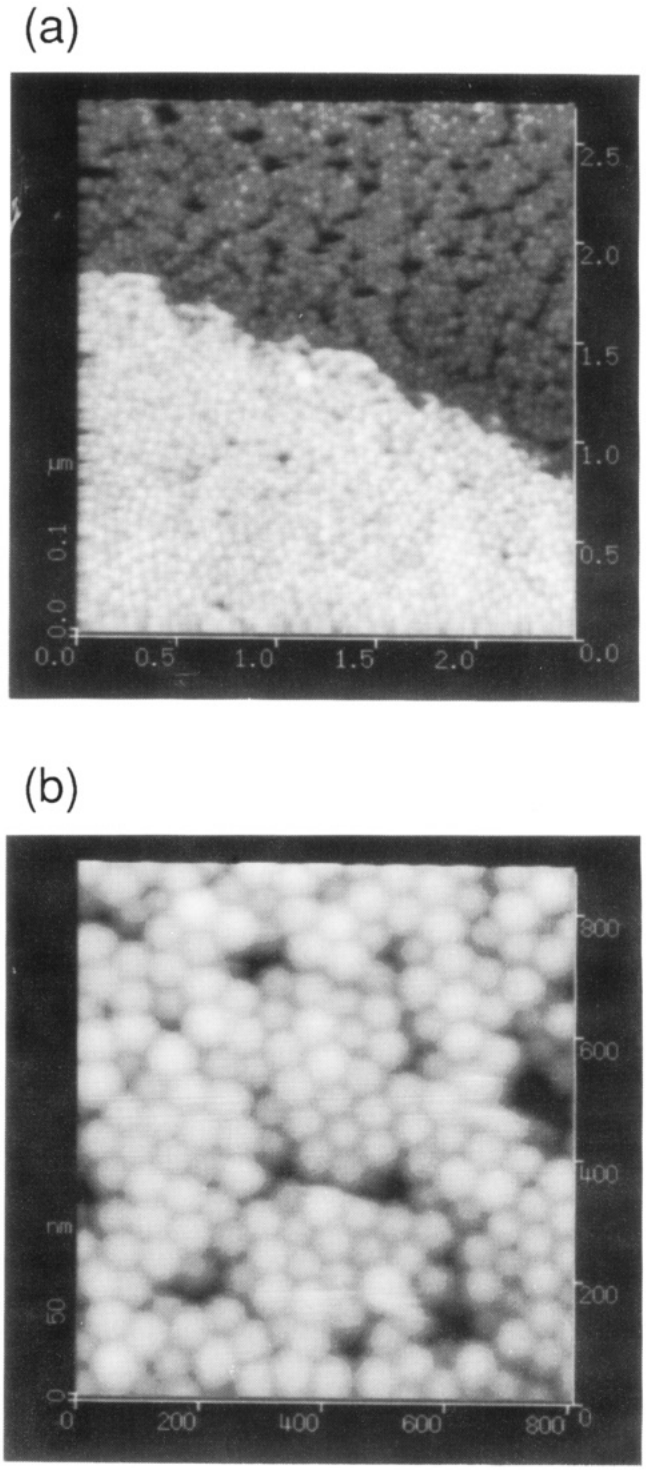

Figure 4. AFM micrographs of layers from latex particles (55 nm diameter) on solid substrate: (a) monolayer and bilayer, normal observation; (b) monolayer at higher magnification.

measurements with latex particle layers deposited on carbon- and gold-coated substrata gave the same λ's in the framework of the experimental precision. This implies that the imaginary part of the refractive index of the gold coating does not affect substantially the occurrence of the observed color phenomenon.

Data Interpretation and Discussion

To interpret the measured $\lambda_{k,k+1}$ let us consider the dependence of the reflectivity, R, of a homogeneous plane-parallel layer on its thickness, h. Note here that the dispersion of the reflectivity R can be ignored, since the *relative* reflective intensity of the successive layers at the *same wavelength* is our concern of analysis. In general,

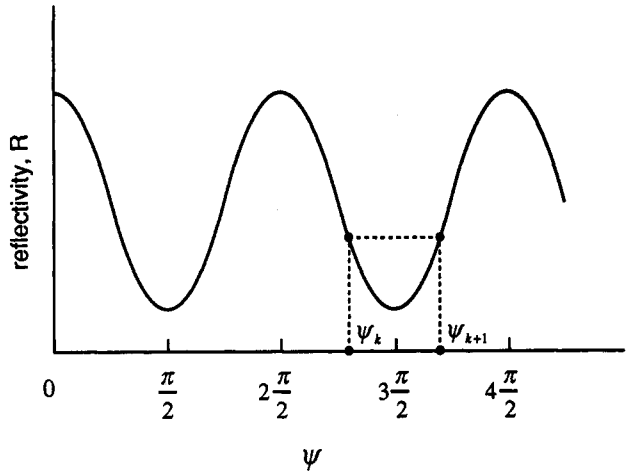

Figure 5. Reflectivity, R, of a thin film on substrate (in arbitrary units) as a function of the phase angle ψ. The figure illustrates eq 3 for $m = 3$.

Table II. Data for Stripes of Coinciding Intensity in Monochromatic Light

k	$\lambda_{k,k+1}$, nm	n_2	m	$f(k)$	$\Lambda(k)$, nm
	(1) Particle Diameter d = 55 nm				
2	581	1.398	1	3.00	207
3	415	1.432	2	5.00	289
4	524	1.424	2	7.00	367
5	625	1.421	2	9.00	439
5	425	1.442	3	9.00	442
6	495	1.435	3	11.00	517
7	563	1.431	3	13.00	590
8	629	1.428	3	15.00	661
8	481	1.441	4	15.00	667
9	534	1.436	4	17.00	743
10	585	1.433	4	19.00	816
11	525	1.439	5	21.00	912
	(2) Particle Diameter d = 144 nm				
1	524	1.366	2	1.01	378
2	560	1.400	3	3.00	597
3	583	1.412	4	5.00	824
4	592	1.419	5	7.00	1042

R depends on h through the phase angle[12,22]

$$\psi = \frac{2\pi}{\lambda} h(\epsilon_2 - \sin^2 \vartheta_0)^{1/2} \tag{1}$$

where λ is light wavelength *in air*, θ_0 is the angle of incidence, and ϵ_2 is the dielectric permittivity of the layer (medium 2), which is situated between medium 1 (air) and medium 3 (substrate). In our case medium 2 (the dried latex multilayer) is transparent and hence $\epsilon_2 = n_2^2$, where n_2 is the respective refractive index. If the substrate is also transparent, R depends on ψ through $\sin^2 \psi$; see, e.g., ref 12 or 22. Hence R is a periodical function of ψ, as sketched in Figure 5. For normal incidence $\theta_0 = 0$ and eq 1 yields

$$\psi_k = \frac{2\pi}{\lambda} h_k n_2 \tag{2}$$

where h_k is the thickness of a multilayer built up from k particle layers and n_2 is an effective refractive index of the multilayer treated as a continuous medium (for model calculation of n_2, see below). As shown in Figure 5, a sufficient condition for $R(\psi_k) = R(\psi_{k+1})$ is

$$m\frac{\pi}{2} - \psi_k = \psi_{k+1} - m\frac{\pi}{2} \tag{3}$$

$$m = 1, 2, 3, \ldots$$

For an even (odd) value of m the intensities of the two neighboring stripes, k and $k+1$, will coincide in the vicinity of an interference maximum or minimum. By substituting eq 2 into eq 3 one obtains

$$\frac{m}{2}\lambda_{k,k+1} = h_k n_2(k) + h_{k+1} n_2(k+1) \tag{4}$$

where the dependence of the effective refractive index n_2 on the layers number k is also taken into account. One can assume that[8]

$$n_2(k) = n_p \varphi_p(k) + [1 - \varphi_p(k)] \tag{5}$$

where n_p and φ_p are the particle refractive index and volume fraction; the refractive index of interparticle medium (air) is set equal to 1. For polystyrene n_p is given by the equation[8,24]

$$n_p = 1.5683 + \frac{1.0087 \times 10^{-10}}{\lambda^2} \tag{6}$$

with λ in cm. The volume fraction φ_p depends on the structure of the multilayer. A monolayer of *hexagonal* close packing can induce multilayer formation having three-dimensional hexagonal close packing (hcp) or face centered cubic lattice (fcc). In both cases simple geometrical considerations yield

hcp:
$$\varphi_k = \frac{\pi k}{3[3^{1/2} + (k-1)2^{1/2}]} \tag{7}$$

$$k = 1, 2, 3, \ldots$$

On the other hand, a monolayer of *square* packing can induce formation of body centered *tetragonal* lattice of *close packing* (tcp). In this case

tcp:
$$\varphi_k = \frac{\pi k}{3[2 + (k-1)2^{1/2}]} \tag{8}$$

$$k = 1, 2, 3, \ldots$$

Values of n_2 calculated by means of eqs 5–7 for the respective k and $\lambda_{k,k+1}$ are presented in Table II. In general n_2 depends on k through φ_p, eq 7, and on λ through n_p, eq 6. If the dependence on λ were negligible, n_2 in Table II would monotonously increase with the increase of k. However, a glance at Table II shows that the effects of k and λ on n_2 are of comparable magnitude for the 55-nm latex.

By setting $n_2(k) \approx n_2(k+1) \approx n$, $h_k \approx ks$, and $h_{k+1} \approx (k+1)s$ in eq 4 it is easy to estimate

$$s \approx m\lambda_{k,k+1}/[2(2k+1)\bar{n}] \tag{9}$$

$$k = 1, 2, 3, \ldots$$

where the quantity s must be close to the particle diameter, d, and $\bar{n}$ is some mean value of n_2, say $n = 1.4$; cf. Table II. By using eq 9 from the data for k and $\lambda_{k,k+1}$, one can determine the interference order m. (For each k and $\lambda_{k,k+1}$ there is only one integer m giving s close to d.) The values of m thus determined are listed in Table II.

(22) Landau, L. D.; Lifshiz, E. M. *Electrodynamics of Continuous Medium*; Pergamon Press: Oxford, 1960.
(23) Bateman, J. B.; Weneck, E. J.; Eshler, O. C. *J. Colloid Sci.* **1959**, *14*, 308.
(24) McDonald, S. A.; Daniels, G. A.; Davidson, J. A. *J. Colloid Interface Sci.* **1977**, *59*, 342.

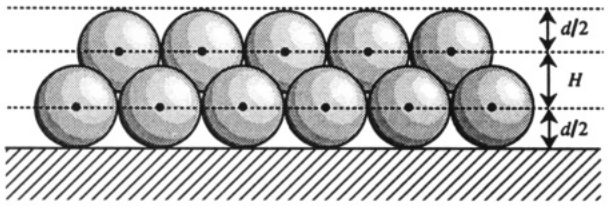

Figure 6. Sketch of a closely packed bilayer on substrate: d is particle diameter; H is the height of a pyramid whose vertices are located in the centers of the respective neighboring particles.

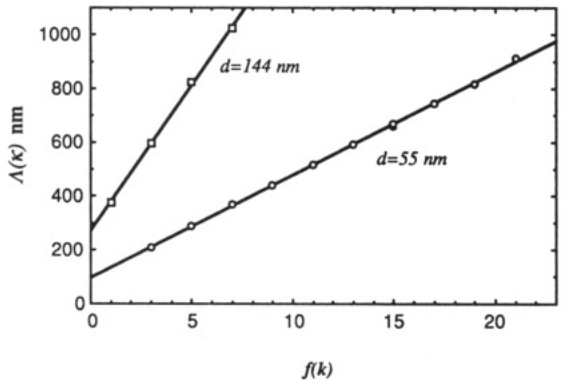

Figure 7. Plot of $\Lambda(k)$ vs $f(k)$; the interferometric data for the two kinds of particles are listed in Table II.

Geometrical considerations illustrated in Figure 6 lead to the conclusion that the thickness of a closely packed multilayer can be represented in the form

$$h_k = d + (k-1)H \tag{10}$$

$$k = 1, 2, 3, \ldots$$

The distance, H, between two neighboring layers in a multilayer depends on the type of lattice:

$$H = \begin{cases} d(2/3)^{1/2} \text{ for hcp} \\ d/2^{1/2} \text{ for tcp} \end{cases} \tag{11}$$

By substitution from eq 10 one can transform eq 4 to read

$$\Lambda(k) = 2d + Hf(k) \tag{12}$$

where

$$\Lambda \equiv \frac{m\lambda_{k,k+1}}{2\bar{n}_2(k)} \tag{13}$$

$$f(k) \equiv \frac{(k-1)n_2(k) + kn_2(k+1)}{\bar{n}_2(k)} \tag{14}$$

$$\bar{n}_2(k) \equiv \frac{1}{2}[n_2(k) + n_2(k+1)] \tag{15}$$

$n_2(k)$ is to be calculated from eqs 5–7. The values of $\Lambda(k)$ and $f(k)$ are shown in Table II. One sees that because of the small variations of $n_2(k)$ in fact $f(k) \approx 2k - 1$.

In accordance with eq 12 the plot of $\Lambda(k)$ vs $f(k)$ must be a straight line. In addition, for this line

$$\frac{\text{intercept}}{\text{slope}} = \frac{2d}{H} = \begin{cases} 6^{1/2} \text{ for hcp} \\ 8^{1/2} \text{ for tcp} \end{cases} \tag{16}$$

cf. eq 11. Our data for $\Lambda(k)$ vs $f(k)$ plotted in Figure 7 correlate very well with a straight line. The ratio intercept/slope (see Table III) for both lines is close to $\sqrt{6} = 2.45$ and noticeably less than $\sqrt{8} = 2.83$. In view of eq 16 this result means that the interferometric data for $\Lambda_{k,k+1}$ are in agreement with the hcp rather than with the tcp lattice. This finding is consonant with the SEM and AFM micrographs in Figures 3 and 4. (As mentioned above, tcp-lattice can be sometimes observed at the boundary between two successive hcp multilayers, Figure 3a; however the area covered with tcp is negligible.)

Table III. Parameters of the Straight Lines in Figure 7

d, nm according to producer	slope, nm	intercept/slope	correlation coefficient	d, nm determined from slope
55	38.3 ± 0.5	2.47 ± 0.14	0.9997	47 ± 0.6
144	111.1 ± 0.5	2.39 ± 0.02	0.99997	136 ± 0.6

The effective particle diameter, d, determined from the slope (Table III) turns out to be lower than the value of d provided by the producer. This is not surprising and can be attributed to the presence of cracks and other defects in the ordered multilayers observed in the micrographs, Figures 2–4. Indeed, our model considerations, especially eq 10, correspond to a perfect lattice, which however is not the real experimental situation. The decrease in the averaged particle volume fraction due to the cracks appears as an effective decrease of the particle diameter as determined from the slope of the lines in Figure 7. The shrinking of the latex particles after the water evaporation[24] could also contribute to this result, especially if the producer has determined d by means of light scattering from the particles inside an aqueous suspension.

Concluding Remarks

The latex particle ordered multilayers of different thicknesses exhibit different uniform colors when illuminated with polychromatic light. The intensity of the colors can be considerably increased by coating the substrate with carbon or gold thin film before latex deposition.

Interferometric measurements in monochromatic light confirm the hypothesis that the colors are due to interference at plane parallel films (the multilayers). The interferometric data processed by means of eq 12 provide information about the structure of the latex array. In particular, they allow one to distinguish between lattices of hexagonal and tetragonal packing. These results as well as the SEM and AFM micrographs reveal that the latex multilayers have predominantly hexagonal packing. Dislocations and cracks are observed in the lattice. These defects, however, are not visible with optical microscopy in the case of the smaller latex particles (55 nm) studied by us. The domains of different lattice orientations but of the same packing and thickness exhibit the same interference color. (If the particles were bigger, say larger than 0.4 μm, such domains would exhibit different iridescence colors due to Bragg reflectance diffraction.[2,8])

The main contributions of the presented study can be summarized as follows:

(i) By use of a special technique, multistepwise latex particle structure is formed.

(ii) It is observed that each step of uniform thickness exhibits an uniform color due to light interference at a plane parallel film; the physical origin of the colors is confirmed quantitatively—cf. eq 12 and Figure 7.

(iii) It is established that in spite of the small size of the particles (diameter far smaller than the wavelength of the visible light), the *light* interferometric data bring information about the layers *structure*—cf. eq 16 and Table III.

(iv) A comparison with the literature[25] shows that the AFM micrographs, Figure 4, demonstrate the best instrumental resolution achieved with this method for latex particle structures up to now.

We hope that a further development of the technique for latex particle array preparation will enable one to obtain larger ordered multilayers of constant thickness, exhibiting uniform colors. The main feature of such a multilayer is the sharp transition from one to another color when removing the upper layer of particles. This could be done by means of AFM or other precise micromanipulation technique. In principle this property of the latex particle multilayers can be utilized for recording colored images of micrometer scale size.

(25) Wang, Y.; Juhne, D.; Winnik, M. A.; Leung, O. M.; Goh, M. C. *Langmuir* **1992**, *8*, 760.

Acknowledgment. This work was supported by the program "Exploratory Research for Advanced Technology" (ERATO), Research and Development Corporation of Japan (JRDC). The authors are grateful to Drs. H. Yoshimura and G. Picard for the illuminative discussion, to Ms. M. Yamaki for the scanning election micrographs, and to Mrs. N. Dushkina for the help in the optical study.